J. Electrical Systems 20-3 (2024): 1287-1298

[1]Ankhi Gulati

[2]Navneet Kumar

[3]Anil Kumar

A Novel Approach for Dynamic Analysis of Wind-Integrated Multi-Machine Power Systems

Journal of Electrical Systems

Abstract: - Indeed, the rapid expansion of Renewable Energy Sources (RES) in recent years has brought about numerous benefits, including reduced carbon emissions, increased energy independence, and the creation of new economic opportunities. However, integrating these variable and intermittent sources into existing power systems poses several challenges for power system management. Faults in electrical networks are among the key factors and sources of network disturbances. Control and automation strategies are among the key fault clearing techniques responsible for the safe operation of the system. In recent years, the increasing penetration of wind energy in multi-machine power systems has posed unique challenges to power grid stability and reliability. Accurate assessment methodologies are required to ensure the effective integration of wind energy sources while maintaining grid stability. Several researchers have revealed various constraints of control and automation strategies such as a slow dynamic response, the inability to switch the network on and off remotely, a high fault clearing time and loss minimization. It's important to note that the impact of wind energy on system inertia is a complex and dynamic aspect of power system operation. Ongoing research and technological advancements aim to improve the integration of wind and other renewable energy sources while ensuring grid stability and reliability. As the energy transition continues, addressing these technical challenges is crucial for building a sustainable and resilient power system. In this paper, the influence of doubly-fed induction generator (DFIG) penetration is analyzed to examine the transient stability of power system networks. The concept of a Coupling Strength Index (CSI) derived from Network Structural Characteristics Theory sounds intriguing, especially in the context of identifying critical elements susceptible to the impact of a three-phase fault in a network. The investigation involves studying the transient stability of a power system under different conditions, specifically with and without doubly-fed induction generators (DFIGs) connected to a weak bus. Additionally, a three-phase fault is applied at the middle of the identified weakest line for both the IEEE 9 and 39 bus systems. The investigation of generator speed, rotor angle, and electric power during transient stability analysis provides a holistic view of how a power system responds to disturbances. This information is crucial for ensuring the reliability and stability of the system, especially when studying the integration of renewable energy sources and addressing potential challenges associated with faults and weak buses. This paper presents a pioneering non-iterative framework for dynamically assessing wind energy dominated multi-machine power systems. The proposed framework aims to address the shortcomings of traditional iterative methods, providing a more efficient and reliable approach to power system analysis.

Keywords: Renewable Energy Sources (RES), Doubly-fed induction generator (DFIG), Coupling Strength Index (CSI), Critical Clearing Time (CCT), Point of Common Coupling (PoCC), Wind Energy (WE), Fault ride-through (FRT)

I. INTRODUCTION

More efforts are done in electricity generation from Renewable Energy Sources (RES) due to the high depletion rate of conventional energy sources and increasing environmental concern. Among various RES, Wind Energy (WE) is the most rapidly growing one. The rapid integration of wind energy (WE) into power systems has brought about significant changes in the dynamic behavior of modern grids. The transient stability of power systems has become a critical concern due to the variable nature of wind resources. The conventional iterative-based approaches have limitations in handling the dynamic behavior of wind-dominated systems. To overcome these challenges, a novel non-iterative assessment framework is introduced in this study. Fault ride-through (FRT) control is an essential feature for modern wind turbines, ensuring their stable and reliable operation during grid faults or disturbances. Doubly Fed Induction Generator (DFIG) wind turbines are one of the most widely used technologies in the wind power industry.

[1] * Research Scholar, Department of Electrical Engineering, School of Engineering & Technology, IFTM University, Lodhipur Rajpoot, Moradabad, Uttar Pradesh, India.

Email id: ankhigulati91@gmail.com

[2] Assistant Professor, Department of Electrical Engineering, Rajkiya Engineering College, Chandpur, Bijnor, Uttar Pradesh, India.

Email id: navneet.ee@recb.ac.in

[3] Professor & Head, Department of Electrical Engineering, School of Engineering & Technology,IFTM University, Lodhipur Rajpoot, Moradabad, Uttar Pradesh, India.

Email id: anilbajuwa@gmail.com

This study aims to comprehensively analyze the influence of wind energy on power system transient stability and identify potential challenges and solutions for maintaining grid stability during dynamic events. Different types of power system instability exist, and their assessments are usually carried out using different approaches. The approaches usually employed in analyzing power system instability depend on the criticality of the faults in the system [1]. Recently, the study of the influence of Wind Energy on power system transient stability is an important aspect of power system analysis and planning, particularly as renewable energy sources like wind power are becoming increasingly integrated into the electricity grid. Transient stability refers to the ability of a power system to maintain synchronism and recover its steady-state operating condition following a disturbance, such as a fault or sudden changes in load [2]. It is a critical characteristic of a power system to ensure the reliable and secure operation of the grid. Steady state stability studies are concerned with the small and gradual changes in the system operating conditions. As such, is significant to determine the Critical Clearing Time (CCT) of the system as this serves as a crucial metric in determining the network stability during transient stability assessment [3].

When wind energy is added to a power system, it introduces certain challenges due to its inherent variability and uncertainty. Wind power generation depends on meteorological conditions, which can change rapidly, causing fluctuations in the power output from wind farms. These fluctuations can affect the overall stability of the power system. Here are some key aspects studied in relation to wind energy's influence on power system transient stability:

1. Modeling Wind Farms: Wind farms need to be accurately represented in power system models to simulate their impact on the grid. Different types of wind turbines and control strategies affect the dynamic behavior of the power system differently.

2. Power System Stability Analysis: Conducting transient stability analysis involves simulating various transient events, such as faults, and evaluating the system's response in the presence of wind energy. This helps identify potential stability issues and necessary control measures.

3. Control and Grid Integration Strategies: Advanced control strategies for wind turbines and wind farms can be employed to enhance transient stability. For instance, grid codes and regulations may require wind farms to have certain features to support system stability during faults.

4. Grid Code Compliance: Many countries have grid codes and regulations that define the requirements for wind power plants to ensure the stability and reliability of the grid during both normal and abnormal conditions.

5. Synchronous Condensers and Energy Storage: The integration of synchronous condensers and energy storage systems can enhance transient stability by providing additional grid support during disturbances and variations in wind power output.

6. Dynamic Voltage Support: Wind farms can be designed with control capabilities to provide dynamic voltage support during transient events, contributing to system stability.

7. Impact of Wind Power Forecasting: Accurate wind power forecasting can help grid operators better anticipate fluctuations in wind power output, allowing for improved system planning and coordination.

8. Resilience and Black Start Capability: Assessing the resilience of the power system with a significant share of wind energy and ensuring its ability to recover after a blackout or system-wide disturbance is crucial.

Overall, the study of the influence of wind energy on power system transient stability is vital to ensure the smooth integration of renewable energy sources into the grid without compromising the overall stability and reliability of the power system [5]. It helps power system engineers and operators make informed decisions and implement appropriate measures to address the challenges posed by the variability of wind power and maintain grid stability under various operating conditions.

II. Literature Review

This explains why some countries are coming up with different plans regarding RES integration in such a way as to reduce the use of fossil fuel in energy stations to the barest minimum [4]. Due to the energy transition, most of the renewable energy in the world is generated using wind power which tends to decrease the inertia of the grid. To protect the integrity of the grid operation in terms of stability and reliability, it is critical to assess the impact of such wind energy systems on transient stability. Faults are inevitable and cannot be eliminated within the system in practice. However, it is usually expected that whenever a small or large disturbance in the form of faults or load variations occurs, the system must be able to adjust rapidly and guarantee optimal performance [6]. Despite the advantages of combining cutting-edge power plant technology, the expanding usage of renewable energy sources offers substantial operational challenges for power systems. In resolving the transient stability issues in a power network integrated with RES, various contributions have been made in the open literature. For instance, [6] investigates the effects of wind energy on a small test power system. When wind power penetration in a power system is large, the load ability of such a network could be reduced. Addressing the risk of voltage instability in the context of weak transmission networks requires a holistic approach involving technology, infrastructure investment, grid planning, and supportive policies. As renewable energy integration continues to grow, ensuring the stability of power systems becomes paramount for a reliable and sustainable energy future [7]. Due to the intermittency nature of RES, power systems integrated with wind power plants may experience transient instability. This could be traced to the interactions that exist between the control systems of wind power generators and the control systems of conventional power plants [8]. Power network management and control have been hampered by the fast improvement of power conversion technologies in wind power facilities [9]. Additionally, the usage of an asynchronous generator mandates the use of network reactive power. As a result, reactive power flow and voltage stability may be affected. For wind power facilities with high penetration, a robust control algorithm is required to ensure energy supply continuity and power system transient stability [10]. It has been shown that a good choice for wind turbines is the Doubly-Fed Induction Generator (DFIG) and its full usage in power systems has been documented in the literature [11,12,13]. The DFIG's dynamic response is primarily reliant on the converters coordinated control techniques [14,15]. The impacts of integrating DFIG into the power system on the system's transient stability have been thoroughly investigated. For instance, Elkington et al, [16] represents an advanced and comprehensive approach to enhancing the stability of power systems with significant wind energy integration by using power system stabilizer (PSS) that combines Eigenvalue analysis and numerical simulations to regulate the impact of DFIG on the network transient stability. In [17], the damping efficacy of the Queensland Transmission system with high penetration of wind power plant was investigated. The choice between variable-speed and fixed-speed wind generators involves trade-offs in terms of efficiency, grid integration, maintenance, and overall system performance. As technology advances and variable-speed solutions become more cost-effective, they are becoming the preferred choice for new wind power installations by Nunesetal. in [18]. Establishing the influence of integrated DFIGs on the system's transient dynamics, the authors of [19] examined the characteristic of transient stability across wind farms based on DFIG penetrations, network topologies, and Point of Common Coupling (PoCC). [20] studied the use of synchro phasor measurements in estimating the equivalent inertia of the wind turbine generators required to detect the angle instability of a system due to the integration wind power integration. Based on the foregoing, this paper attempts to investigate the influence of DFIG-based wind energy penetration on the transient stability of a power network. Another contribution offered by this study lays in the application of a non-iterative based method of Coupling Strength Index (CSI) for quick detection of the most vulnerable transmission line whose removal or outage during fault could be highly detrimental to the system operation. Traditionally, this identification is carried out by using various existing iterative procedures, whose results could be misleading due to associated challenges such as convergence problems, the complexity of Jacobian matrix factorization and refactorization, etc. Consequently, CSIs are characterized by computational time saving as well as a reduction in the computer memory required.

III. MATHEMATICAL FORMULATIONS

Considering a typical interconnected multi-node power network shown in figure 1. Certainly, Ohm's Law is fundamental in understanding the relationship between voltages, currents, and impedances in an electrical network, and a pi equivalent model is a common representation for transmission lines and is expressed as,

$$I_{bus}=Y_{bus}V_{bus} \tag{1}$$

Alternatively, at any bus i,

$$I_i=\sum_{j=1}^{n} Y_{ij}V_j \tag{2}$$

where, Y_{ij} is the mutual admittance of the transmission line between buses *i* and *j* and V_j represents bus *j* voltage. The complex apparent power (S) at any bus in an electrical power system is expressed as the product of the bus voltage (V) and the complex conjugate of the bus current (I). Mathematically, it can be represented as follows:

$$S_i = P_i + jQ_i = V_j \times I^*_{IJ} \tag{3}$$

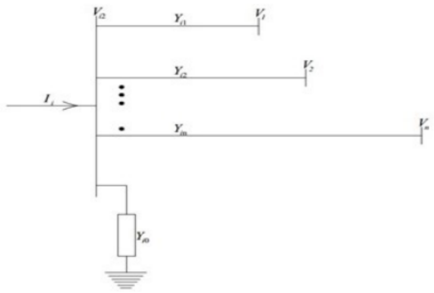

Figure 1: A Multi-Node Power Network

Algebraic manipulations of (2) and (3) results in the power-flow equations given by

$P_i = \mathrm{Re}\{\sum_{j=1, j\neq i}^{n} Vi * Vj * Yij\}$ (4)

$Q_i = -\mathrm{Im}\{\sum_{j=1, j\neq i}^{n} Vi * Vj * Yij\}$ (5)

Assuming the n-bus network shown in Fig. 1 in a power system with n buses and g generators (where n>g) a pre-fault load-flow analysis provides the steady-state operating conditions of the network, then at any bus *i*, the vector of network voltages, (V_i), generator active powers, (P_{gi}), and generator reactive powers (Q_{gi}), then (E_i) can be given by

$$E_i = V_i + jX_i \frac{Pgi - jQgi}{Vi*} \quad (6)$$

When transforming a load bus to its corresponding constant admittance form Y_{LI}, the equivalent reactance X_i at bus *i* is used to represent the reactive power injection at that bus.

$Y_{LI} = (P_{LI} - JQ_{Li})/|V_i|^2$ (7)

$Y_{bus} = \begin{bmatrix} Ygg & Ygl \\ Ylg & Yll \end{bmatrix}$ (8)

Certainly, let's proceed with the development of the pre-fault partitioned bus admittance matrix Y_{bus} incorporating generator reactance X_i, real power P_{LI}, and reactive power Q_{LI} at each load node. The pre-fault partitioned bus admittance matrix Y_{bus} is typically divided into four submatrices: Y_{ll}, Y_{lg}, Y_{gl} and Y_{lg}. The indices *l* and *g* represent load and generator buses, respectively.

Assuming no damping effect, the swing equation can be formulated as follows:

$\frac{H}{\pi f} d^2\delta_i/dt^2 = P_{mi} - E_I^2 Y_{ii}\cos\theta_{ii} - \{\sum_{j=1, j\neq i}^{n} |Ei| * |Ej| * |Yij| * \cos(\delta_j - \delta_i + \theta_{ij})\}$ (9)

where

δ = phase angle of the bus voltage

θ = admittance angle

Let's express the swing equation during a fault condition:

$\frac{H}{\pi f} d^2\delta_i/dt^2 = P_{mi} - P_{ei\ (during\ fault)}$ (10)

For the post-fault conditions, the swing equation can be expressed as

$\frac{H}{\pi f} d^2\delta_i/dt^2 = P_{mi} - P_{ei\ (after\ fault)}$ (11)

The relationship between mechanical power & electrical power can be expressed as follows: [19, 22]:

$P_e = T_m\omega_r$ (12)

$P_s = T_e\omega_s$ (13)

Certainly! The dynamic voltage equations for a Doubly-Fed Induction Generator (DFIG) can be expressed as follows:

1. Stator Voltage Equations:

The stator voltage equations for a DFIG are similar to those of a conventional induction generator. The stator voltage is given by:

$V_s = R_s * I_s + j\omega L_s * I_s + V_t$ (14)

where:

- V_s is the stator voltage.
- R_s is the stator resistance.

- I_s is the stator current.
- ω is the synchronous speed of the generator.
- L_s is the stator leakage inductance.
- V_t is the induced stator voltage due to the rotor magnetic field (this term is related to slip frequency and varies with the rotor speed).

2. Rotor Voltage Equations:

The rotor voltage equations for a DFIG account for the fact that the rotor windings are connected to the power grid through slip rings and can be controlled independently. The rotor voltage is given by:

$V_r = R_r * I_r + j(\omega - \omega_r) * L_r * I_r$ (15)

where:
- V_r is the rotor voltage.
- R_r is the rotor resistance.
- I_r is the rotor current.
- ω_r is the angular speed of the rotor (not necessarily equal to the synchronous speed ω).
- L_r is the rotor leakage inductance.

3. Rotor Speed Equation:

The rotor speed equation relates the difference between the rotor speed and the synchronous speed to the electromagnetic torque generated by the DFIG:

$J * d(\omega_r)/dt = T_e - T_m$ (16)

where:
- J is the moment of inertia of the rotor.
- $d(\omega_r)/dt$ is the rate of change of the rotor speed.
- T_e is the electromagnetic torque generated by the DFIG (determined by the interaction between the stator and rotor currents).
- T_m is the mechanical torque applied to the generator shaft.

These equations, combined with appropriate control strategies and mechanical equations, form a complete dynamic model of a DFIG. The dynamic model is used to analyze the behavior of the DFIG under different operating conditions, including transient and steady-state performance. It helps in understanding and optimizing the control of the generator for various applications, such as wind power generation and grid stabilization.

To represent the dynamic model, these equations can also be written as:

$V_{ds} = R_s i_{ds} - \omega_s \psi_{qs} + \frac{1}{\omega b} d\psi_{ds}/dt$ (17)

$V_{qs} = R_s i_{qs} - \omega_s \psi_{ds} + \frac{1}{\omega b} d\psi_{qs}/dt$ (18)

$V_{dr} = R_r i_{dr} - (\omega_s - \omega_r)\psi_{qr} + \frac{1}{\omega b} d\psi_{dr}/dt$ (19)

$V_{qr} = R_r i_{qr} - (\omega_s - \omega_r)\psi_{dr} + \frac{1}{\omega b} d\psi_{qr}/dt$ (20)

By ignoring turbine and generator self-damping with R_s, R_r representing stator and rotor resistance respectively and represents the flux linkage. The two-mass model is often used to represent the dynamic behavior of the drivetrain in wind turbines. This model considers the interaction between the rotor and the generator, treating them as two separate masses with their associated inertia and damping. The equations that characterize the two-mass model for the drivetrain can be written as follows:

$d\omega_r/dt = \frac{1}{2Hg}(T_{sh}\text{-}T_e\text{-}B\omega_r)$ (21)

$d\omega_t/dt = \frac{1}{2Ht}(T_m\text{-}T_{sh})$ (22)

$d\theta_t/dt = \omega_b (\omega_t - \omega_r)$ (23)

The shaft torque T_{sh}, electromagnetic torque T_e, and mechanical torque T_m can then be expressed as follows:

$T_{sh} = k_{sh}\theta_t + D_{sh}\omega_b (\omega_t - \omega_r)$ (24)

$T_e = L_m (i_{qs}i_{dr} - i_{ds}i_{qr})$ (25)

$T_m = \rho\pi R^2 C_p (\gamma,\beta) v_w^3 / \omega_t$ (26)

where,

R = ratio of the turbine in meters,

C_p = performance coefficient, γ is the tip speed,
β = blade pitch angle, ρ is the air density in kg/m^3 and
v_w = wind velocity in m/s.

IV. Results And Discussion

The standard IEEE 9-bus and IEEE 39-bus networks are used to illustrate the effectiveness of the framework suggested in this study. These networks are used to conduct an assessment of transient stability with a special focus on the penetration of DFIG. The simulations were carried out using DIgSILENT Power Factory, and the data was extracted and plotted using Python's mat-plotlib library. The problem was dynamically modeled in the 3rd order of three conventional generators, each fitted with an IEEE X1 exciter and a PSS2A stabilizer. Using the Coupling Strength Index (CSI) to identify the weakest line in a power network without requiring iteration is a valuable approach for fault location determination. Table 1 presents the implementation of the CSI method using the network model of the IEEE 9-bus system and analysis of the results has been done accordingly. Determining the Coupling Strength Index (CSI) for all transmission lines in a power system and then ranking them based on decreasing order of magnitudes is the approach to identify the weakest links in the network. For example, the CSI value for the line connecting buses 7 and 8 within the load-to-load region is 0.02739, representing the lowest CSI value in the network and is ranked number 1. The next line ranked is the one connecting buses 4 and 5 within the load-to-load attraction region of influence, with a CSI value of 0.02275, ranked number 2, and so on. The transmission line that connects nodes 7 and 8 is therefore identified as the weakest line, where the influence of the fault will be most critical to the integrity of the grid operation. In table 2, the row with the highest CSI value is row number 9, which represents the CSI value 0.105158 for the line connecting buses from bus 5 to bus 6. A higher criticality index suggests that this particular line is more vulnerable to faults and may have a more significant impact on the overall stability of the power system. The highest CSI value for the line connecting buses is from bus 5 to bus 6 which connects two important buses in the network and has a length of 5 km.

From Bus	***To Bus***	***CSI***	***CSI Ranking***
4	*5*	*0.02275*	*2*
4	*6*	*0.02102*	*3*
5	*7*	*0.01186*	*5*
6	*9*	*0.01128*	*6*
7	*8*	*0.02739*	*1*
8	*9*	*0.0197*	*4*

Table 1: Detection of Weakest Transmission Line for IEEE 9

From Bus	***To Bus***	***CSI***	***CSI Ranking***
1	*2*	*0.000456*	*32*
1	*39*	*0.001216*	*27*
2	*3*	*0.00332*	*22*
2	*25*	*0.006371*	*13*
3	*4*	*0.001603*	*25*
3	*18*	*0.004209*	*17*
4	*5*	*0.00433*	*15*
4	*14*	*0.004293*	*16*
5	*6*	*0.105158*	*1*
5	*8*	*0.005604*	*14*
6	*7*	*0.008346*	*10*
6	*11*	*0.008346*	*7*
7	*8*	*0.032877*	*4*
8	*9*	*0.000546*	*31*
9	*39*	*0.001194*	*28*

10	*11*	*0.038992*	*3*
10	*13*	*0.03903*	*2*
13	*14*	*0.007045*	*12*
15	*16*	*0.008292*	*11*
16	*17*	*0.009451*	*8*
16	*19*	*0.001998*	*24*
16	*21*	*0.00411*	*18*
16	*24*	*0.021645*	*5*
17	*18*	*0.01111*	*6*
17	*27*	*0.002517*	*23*
21	*22*	*0.00389*	*19*
22	*23*	*0.008371*	*9*
23	*24*	*0.000622*	*30*
25	*26*	*0.000746*	*29*
26	*27*	*0.003535*	*20*
26	*27*	*0.003535*	*20*
26	*29*	*0.000198*	*34*

Table 2: Detection of Weakest Transmission Line for IEEE 39

Monitoring the post-fault behavior of the system's generators, including relative speed, rotor angle, and electric power, during simulations provides valuable insights into the transient stability of the power system. The use of Doubly Fed Induction Generators (DFIGs) in these simulations adds complexity and allows for the study of their impact on system dynamics. Results for scenarios involving a three-phase fault on transmission line number 5 of the IEEE 9 bus system and transmission line number 9 of the IEEE 39 bus system for a duration of 0.1 seconds are shown in figures 2 to 13. The transmission line tripped at both ends, each tripping at a distance of 50 percent.

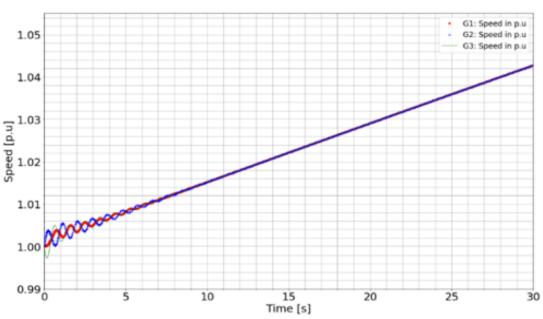

Figure 2: Speed without DFIG for 9 bus system

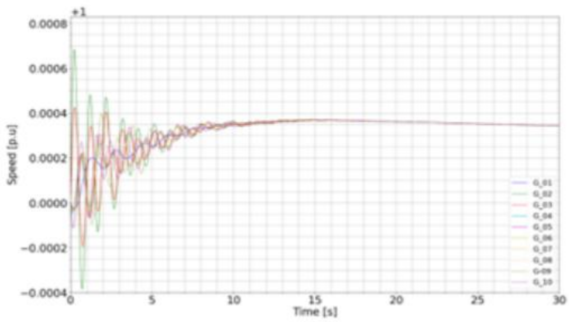

Figure 3: Speed without DFIG for 39 bus system

The simulation results for generators' speed without Doubly Fed Induction Generators (DFIG) for IEEE 9 bus and IEEE 39 bus have been presented in figures 2 and 3, respectively. In both cases, the observation that the mechanical torque and electrical torque of the power system generators are equal at steady state is significant and indicates a balanced operating condition, resulting in a speed of 1.0000 p.u. However, the electrical torque decreased during a three-phase fault, leading to an acceleration in the generators' speed, indicates a transient response in the power system. For IEEE 9 bus, the mechanical torque caused the generators' speed to increase to a value of 1.0427 p.u. On the other hand, for IEEE 39 bus, after the 10 generators had more swings at the first 5 seconds, the mechanical torque caused the generators' speed to accelerate to a value of 1.00118 p.u.

Figures 4 and 5, respectively, show the simulation results for the generators speed with DFIG. The observation that the generator speed drastically decreased following a three-phase fault when Doubly Fed Induction Generators (DFIGs) are integrated suggests a specific response of the power system to the fault. The specific post-fault values for the IEEE 9-bus and IEEE 39-bus power systems after a simulation time of 30 seconds, were 0.7311 p.u and 0.9675 p.u, respectively.

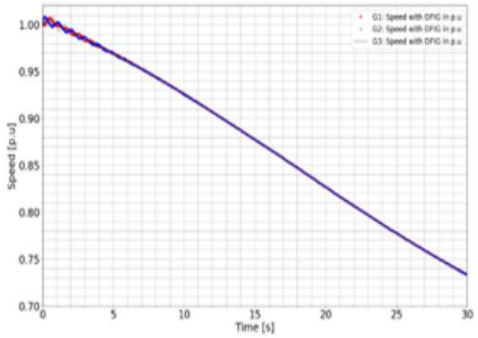

Figure 4: Speed with DFIG for 9 bus system

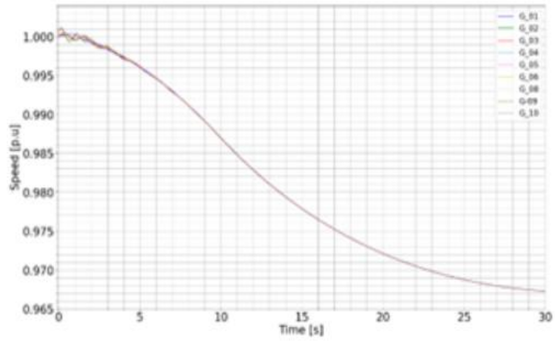

Figure 5: Speed with DFIG for 39 bus system

According to figure 6, during the fault, the rotor angle of generator 2 began oscillating at a value of 41.822 degrees and peaked at 63.168 degrees before stabilizing at 53.026 degrees. In contrast, generator 3’s rotor angle dropped from 37.090 degrees to a steady-state value of 18.039. It can be seen that the scenario without DFIGs experienced less oscillations and that the rotor angle stabilized before the simulation’s 30-second mark. Due to the higher inertia of the system, the generator rotor angles for the IEEE 39 bus in figure 7 did not oscillate as much as they did for the IEEE 9 bus. After five seconds, all ten generators rotor angles stabilized. The higher inertia of the system helps to maintain stability during disturbances such as faults, and the rotor angles return to their steady-state values quickly.

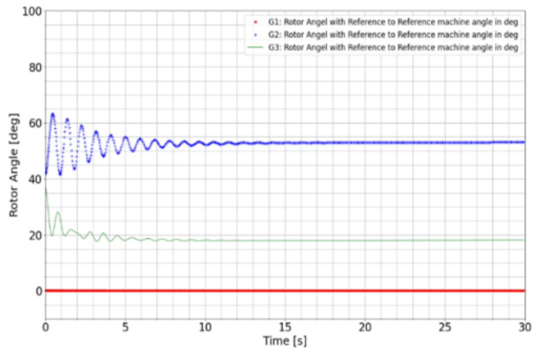

Figure 6: Rotor Angle without DFIG for 9 bus system

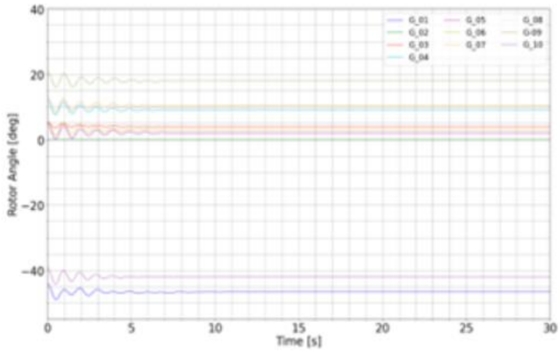

Figure 7: Rotor Angle without DFIG for 39 bus system

The generators rotor angles 2 and 3 in figure 8 remained varied and lost value despite DFIG penetration. The highest value for Generator 2 was 101.2 degrees, which is 59.378 degrees greater than the figure for the first scenario. Due to the penetration of DFIG, the decrease in kinetic energy stored as inertia in the power system which is the source of the minimal variation. The system’s dynamic behavior is impacted by the decrease in kinetic energy, which may cause instability. Although the rotor angle swing in figure 9 for the IEEE 39 bus was not particularly high, it had a significant impact on placement. All generators' rotor angles, except for generator 10, have reduced indicates a change in the angular positions of the generators' rotors. The reason for the decrease in rotor angle is due to the disturbance caused by the fault, which affects the stability of the system. The positioning of the rotor angles is also affected by the penetration of DFIG.

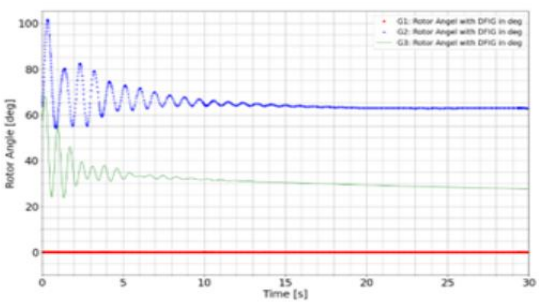

Figure 8: Rotor Angle with DFIG for 9 bus system

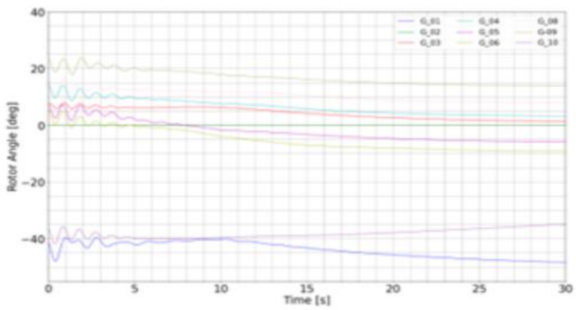

Figure 9: Rotor Angle with DFIG for 39 bus system

The results from figure 10 for IEEE 9 bus indicate that the dependency of the electric power response of each generator on the rotor angle after the three-phase fault. The delay time in reaching a steady-state operation after the fault was different for each generator. It can also be observed that generator 2 had the highest peak value of electrical power while generator 1 had the least value. This difference in peak value could be attributed to the amount of kinetic energy stored in the rotating masses of each generator. Furthermore, in figure 11 for IEEE 39 bus, it can be seen that the electrical power response of all the generators decreased during the fault but eventually return to steady-state operation. The decrease in electrical power is due to the reduction in input mechanical power. Generator 2 to 9 had a per-unit value of 0.8 to 1.0 while generator 1 had a significantly lower value of 0.13, and generator 10 had a value of 0.3. The results obtained for both IEEE 9 and IEEE 39 bus show the importance of considering the impact of the DFIG on the electrical power response and stability of the power system after a fault.

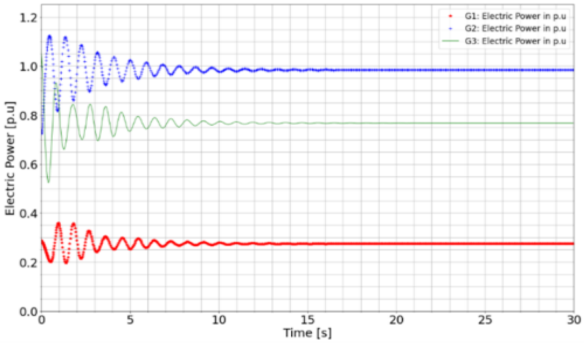

Figure 10: Power without DFIG for 9 bus system

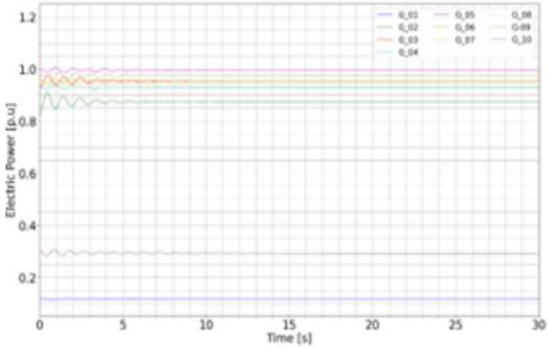

Figure 11: Power without DFIG for 39 bus system

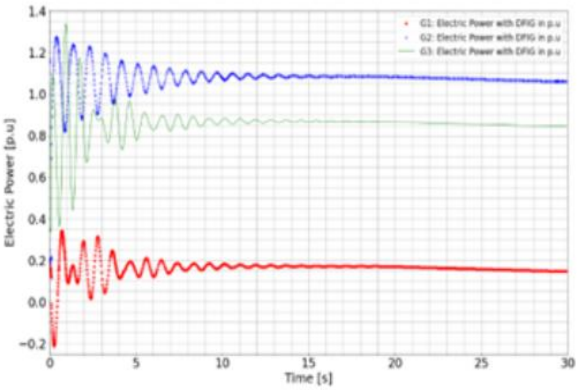

Figure 12: Power with DFIG for 9 bus system

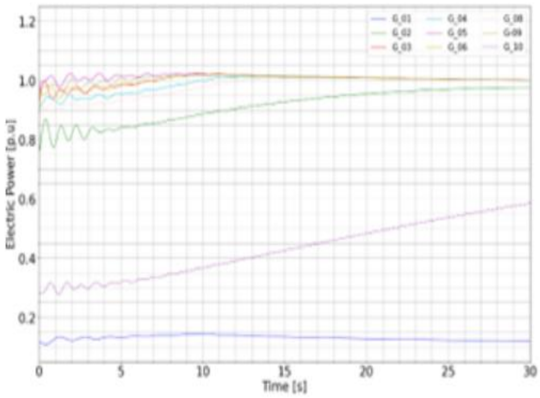

Figure 13: Power with DFIG for 39 bus system

The results of figure 12 and 13 indicate that DFIG penetration affects the system's transient stability in both the IEEE 9 bus and IEEE 39 bus systems. In the case of the IEEE 9 bus system, the observed increase in the peak value of electric power and the resulting fluctuations, including tangential curves in the electric power curves for generators 1 and 3, indicates a dynamic response to a fault or disturbance in the power system. The settling time for the electric power to return to steady state also increased in the presence of DFIGs. Similarly, in the case of the IEEE 39 bus system, the electric power of all generators decreased due to the fault but increased again after 4 seconds to compensate for the load. The reduction in the system's transient stability due to DFIG penetration can be attributed to the reduction in the system's inertia. The kinetic energy stored in the power system as inertia reduces with DFIG penetration, making the system more vulnerable to faults and disturbances. Therefore, the use of DFIGs in power systems requires careful consideration to ensure the system's stability and reliability.

CONCLUSION

Interpreting the simulation results and drawing conclusions about the effects of DFIG penetration on the dynamic stability of the IEEE 9 and 39-bus systems requires a thorough analysis of the obtained data. The following are some general conclusions that might be drawn based on the simulation results:

1. Dynamic Stability Improvement: The simulation results may show that DFIG penetration has a positive impact on the dynamic stability of the power system. With DFIG units contributing to the system's inertia and providing fast-reacting control capabilities, the system may exhibit better post-fault rotor angle and voltage recovery. This improved dynamic stability can be attributed to the enhanced damping and control mechanisms offered by DFIGs.

2. Enhanced Fault Ride-Through Capability: The simulation may reveal that the IEEE 9 and 39-bus systems with higher DFIG penetration levels exhibit improved fault ride-through capabilities. DFIGs can support grid voltage during faults and continue to provide reactive power, contributing to a smoother recovery after disturbances.

3. Critical Clearing Time Analysis: Comparing the critical clearing times for different DFIG penetration levels can be insightful. It might be observed that as DFIG penetration increases, the critical clearing time decreases, indicating a faster post-fault stabilization of the system.

4. Voltage Stability Margin: The simulation results may indicate that higher DFIG penetration levels help maintain better voltage stability margins during transient events. The reactive power support from DFIGs can enhance the voltage profile and mitigate voltage collapse during severe disturbances.

5. Impact on Rotor Angle Stability: Analyzing the rotor angle stability in response to disturbances can reveal the effectiveness of DFIG integration. Higher DFIG penetration levels might result in reduced rotor angle deviations, indicating a more stable system.

6. Trade-offs and Challenges: The results may also uncover potential challenges or trade-offs associated with DFIG integration. For example, increasing DFIG penetration might lead to an increase in system complexity or introduce additional control interactions. These aspects should be carefully considered in the overall power system planning.

7. Optimal DFIG Penetration: Based on the simulation outcomes, it might be possible to identify an optimal DFIG penetration level that balances stability improvement and potential challenges. This optimal level can guide power system planners in determining the suitable proportion of DFIGs in the grid.

8. Sensitivity Analysis: Sensitivity analysis can provide insights into the influence of key parameters like DFIG control settings, location of DFIG units, and system operating conditions on dynamic stability. This information can be valuable for tuning control strategies and system operation.

Overall, the study's conclusions can guide power system operators and planners in making informed decisions about integrating DFIG units into the IEEE 9 and 39-bus systems or similar power grids.

The study provides valuable insights into the effects of DFIGs on the dynamic stability of power systems and highlights the need for improved control strategies to mitigate the negative impacts of DFIGs penetration. The study also explored a faster approach of CSI for identifying the weakest line where a three-phase fault is applied. The research also showed that the stabilization time of electrical power after a fault with DFIG penetration is significantly longer. Furthermore, the rotor angle displayed a variation after DFIG penetration due to the kinetic energy stored in the electrical system as inertia. The comparison of the system's performance with and without DFIGs was observed, and it was concluded that the transient stability of the IEEE 9 and 39 bus system is negatively impacted by DFIGs penetration, with the generator closer to the penetrated DFIGs affected the most. Also, because of lower number of generators and lines the DFIG integration affected the IEEE 9 bus system more than the IEEE 39 bus system for the speed, rotor angle, and electric power which results in a lower level of redundancy in the system. This lower redundancy makes the system more vulnerable to disturbances. Additionally, the IEEE 9 bus system has a lower level of inertia than the IEEE 39 bus system, which reduces its ability to maintain its stability during disturbances. In contrast, the IEEE 39 bus system has a higher number of generators and lines, which provide a higher level of redundancy and stability. Therefore, the integration of DFIGs had a smaller impact on the stability of the IEEE 39 bus system compared to the IEEE 9 bus system.

Acknowledgment

I would like to express my sincere gratitude to Prof. Anil Kumar for his valuable guidance, encouragement and support throughout the research process. His expertise and mentorship have been instrumental in shaping the direction and quality of this work. I also extend my appreciation to Dr. Navneet Kumar for his assistance with analysis and fruitful discussions during group meetings. Furthermore, I extend my sincere gratitude to the individuals and organizations whose support and collaboration have been fundamental to the completion of this research endeavor. Their input has enriched the discussion and outcomes of this study.

REFERENCES

[1] G. S. Lee, D. H. Kwon, and S.il Moon, "DC Current and Voltage Droop Control Method of Hybrid HVDC Systems for an Offshore Wind Farm Connection to Enhance AC Voltage Stability," IEEE Transactions on Energy Conversion, vol. 36, no. 1, pp. 468–479, Mar. 2021, doi: 10.1109/TEC.2020.3005777.

[2] Y. Chi, Y. Xu, and R. Zhang, "Many-objective robust optimization for dynamic VAR planning to enhance voltage stability of a wind-energy power system," IEEE Transactions on Power Delivery, vol. 36, no. 1, pp. 30–42, Feb. 2021, doi: 10.1109/TPWRD.2020.2982471.

[3] W. Olalekan Idris, M. Z. Ibrahim, and A. Albani, "The status of the development of wind energy in nigeria," Energies (Basel), vol. 13, no. 23, Dec. 2020, doi: 10.3390/en13236219.

[4] B. Qin, H. Li, X. Zhang, T. Ding, K. Ma, and S. Mei, "Quantitative Short-Term voltage stability analysis of power systems integrated with DFIG-based wind farms," IET Generation, Transmission and Distribution, vol. 14, no. 19, pp. 4264–4272, Oct. 2020, doi: 10.1049/ietgtd.2019.1701.

[5] B. B. Adetokun, C. M. Muriithi, and J. O. Ojo, "Voltage stability assessment and enhancement of power grid with increasing wind energy penetration," International Journal of Electrical Power and Energy Systems, vol. 120, Sep. 2020, doi: 10.1016/j.ijepes.2020.105988.

[6] Aphrodis Nduwamungu , Etienne Ntagwirumugara , Francis Mulolani and Waqar Bashir , Fault Ride through Capability Analysis (FRT) in Wind Power Plants with Doubly Fed Induction Generators for Smart Grid Technologies; Energies 2020, 13, 4260; doi:10.3390/en13164260.

[7] Qiu, Y.; Feng, Y.; Infield, D. Fault diagnosis of wind turbine with SCADA alarms based multidimensional information processing method. Renew. Energy 2020, 145, 1923–1931. [CrossRef].

[8] N. Gurung, R. Bhattarai, and S. Kamalasadan, "Optimal Oscillation Damping Controller Design for LargeScale Wind Integrated Power Grid," in IEEE Transactions on Industry Applications, Jul. 2020, vol. 56, no. 4, pp. 4225–4235. doi: 10.1109/TIA.2020.2988432.

[9] S. D. Tavakoli, E. Prieto-Araujo, E. S´anchez-S´anchez, and O. Gomis-Bellmunt, "Interaction assessment and stability analysis of the MMC-based VSC-HVDC link," Energies (Basel), vol. 13, no. 8, Apr. 2020, doi: 10.3390/en13082075.

[10] F. Irtiaz Khan and T. Aziz, "Transient Stability evaluation of a Solar PV Integrated Industrial Microgrid."

[11] A. A. Attabo, O. O. Ajayi, and S. O. Oyedepo, "Wind energy generation from Nigeria continental shelf: A review," in IOP Conference Series: Earth and Environmental Science, Oct. 2019, vol. 331, no. 1. doi: 10.1088/1755-1315/331/1/012019.

[12] M. Eidiani and H. Teimoori, "Transient Stability Analysis of Power Grid in the Presence of Asynchronous Generators using Potential Energy Boundary Surface PEBS," 2019.

[13] S. Oh, H. Shin, H. Cho, and B. Lee, "Transient impact analysis of high renewable energy sources penetration according to the future Korean power grid scenario," Sustainability (Switzerland), vol. 10, no. 11, Nov. 2018, doi: 10.3390/su10114140.

[14] Ibrahim, A.; Solomin, E.; Miroshnichenko, A. Control Strategy for Maximum Power Point Tracking of Doubly Fed Induction Motor for Wind Turbine. In Proceedings of the 2018 International Ural Conference on Green Energy (UralCon), Chelyabinsk, Russia, 4–6 October 2018; pp. 14–19.

[15] Dhouib, B.; Kahouli, A.; Abdallah, H.H. Dynamic behavior of grid-connected fixed speed wind turbine based on proportional-integral pitch controller and fault analysis. In Proceedings of the 2017 International Conference on Green Energy Conversion Systems (GECS), Hammamet, Tunisia, 23–25 March 2017; pp. 1–7.

[16] A. S. Alayande, A. A. Jimoh, and A. A. Yusuff, "Identification of critical buses and weak transmission lines using inherent structural characteristics theory," in Asia-Pacific Power and Energy Engineering Conference, APPEEC, Jan. 2016, vol. 2016-January. doi: 10.1109/APPEEC.2015.7380974.

[17] A. A. B. Mohd Zin, M. H. A. Pesaran, A. B. Khairuddin, L. Jahanshaloo, and O. Shariati, "An overview on doubly fed induction generators controls and contributions to wind-based electricity generation," Renewable and Sustainable Energy Reviews, vol. 27. Elsevier Ltd, pp. 692–708, 2013. doi: 10.1016/j.rser.2013.07.010.

[18] Y. Zhang, J. Bank, E. Muljadi, Y. H. Wan, and D. Corbus, "Angle instability detection in power systems with high-wind penetration using synchrophasor measurements," IEEE Journal of Emerging and Selected Topics in Power Electronics, vol. 1, no. 4, pp. 306–314, Dec. 2013, doi: 10.1109/JESTPE.2013.2284255.

[19] Marwa Ezzat, Mohamed Benbouzid, S.M. Muyeen and Lennart Harnefors; Low Voltage Ride Through Techniques for DFIG Based Wind Turbines: State of the Art Review and Future Trends, IEEE IECON 2013, Vienne, Austria (2013).

[20] N. H. P. R Sharma, "Transient Stability Analysis of Power System Using Matlab," 2012.

[21] H. Li, B. Zhao, C. Yang, H. W. Chen, and Z. Chen, "Analysis and estimation of transient stability for a grid-connected wind turbine with induction generator," Renew. Energy, vol. 36, pp. 1469–1476, 2011, doi: 10.1016/j.renene.2010.08.023.

[22] M. Rahimi and M. Parniani, "Dynamic behavior analysis of doubly-fed induction generator wind turbines - The influence of rotor and speed controller parameters," International Journal of Electrical Power and Energy Systems, vol. 32, no. 5, pp. 464–477, Jun. 2010, doi: 10.1016/j.ijepes.2009.09.017.

[23] O. Ajayi, “The potential for wind energy in Nigeria,” Wind Engineering, vol. 34, no. 3, pp. 303–312, May 2010, doi: 10.1260/0309-524X.34.3.303.

[24] K. Elkington, V. Knazkins, and M. Ghandhari, “On the stability of power systems containing doubly fed induction generator-based generation,” Electric Power Systems Research, vol. 78, no. 9, pp. 1477–1484, Sep. 2008, doi: 10.1016/j.epsr.2008.01.006.

[25] H. Li, B. Zhao, C. Yang, H. W. Chen, and Z. Chen, “Analysis and estimation of transient stability for a gridconnected wind turbine with induction generator,” Renewable Energy, vol. 36, no. 5, pp. 1469–1476, May 2011, doi: 10.1016/j.renene.2010.08.023.

[26] M. V. A. Nunes, J. A. P. Lopes, H. H. Z¨urn, U. H. Bezerra, and R. G. Almeida, “Influence of the variable-speed wind generators in transient stability margin of the conventional generators integrated in electrical grids,” IEEE Transactions on Energy Conversion, vol. 19, no. 4, pp. 692–701, Dec. 2004, doi: 10.1109/TEC.2004.832078.

[27] J. B. Ekanayake, S. Member, L. Holdsworth, X. Wu, N. Jenkins, and S. Member, “Dynamic Modeling of Doubly Fed Induction Generator Wind Turbines,” IEEE Trans. POWER Syst., vol. 18, no. 2, pp. 803–809, 2003.